



OPEN

SUBJECT AREAS:

ELECTRONIC PROPERTIES
AND MATERIALS

NANOTUBES

ELECTRONICS, PHOTONICS AND
DEVICE PHYSICS

ELECTRONIC STRUCTURE

Received

7 March 2013

Accepted

2 September 2013

Published

24 September 2013

Correspondence and
requests for materials
should be addressed to
A.R. (angel.rubio@
ehu.es)

Efficient Gate-tunable light-emitting device made of defective boron nitride nanotubes: from ultraviolet to the visible

Claudio Attaccalite¹, Ludger Wirtz^{2,3}, Andrea Marini⁴ & Angel Rubio^{5,6}

¹Institut Néel, CNRS, 25 rue des Martyrs BP 166, 38042 Grenoble cedex 9 France, ²Institute for Electronics, Microelectronics, and Nanotechnology (IEMN), CNRS UMR 8520, Dept. ISEN, 59652 Villeneuve d'Ascq Cedex, France, ³Physics and Materials Science Research Unit, University of Luxembourg, 162a ave. de la Faiencerie, L-1511 Luxembourg, ⁴Istituto di Struttura della Materia (ISM), Consiglio Nazionale delle Ricerche, Via Salaria Km 29.5, CP 10, 00016 Monterotondo Stazione, Italy, ⁵Nano-Bio Spectroscopy Group and ETSF Scientific Development Centre, Departamento de Física de Materiales, Centro de Física de Materiales CSIC-UPV/EHU-MPC and DIPC, Universidad del País Vasco UPV/EHU, Av. Tolosa 72, E-20018 San Sebastián, Spain, ⁶Fritz Haber Institut der Max Planck Gesellschaft, Faradayweg 4–6, 14195, Berlin, Germany.

Boron nitride is a promising material for nanotechnology applications due to its two-dimensional graphene-like, insulating, and highly-resistant structure. Recently it has received a lot of attention as a substrate to grow and isolate graphene as well as for its intrinsic UV lasing response. Similar to carbon, one-dimensional boron nitride nanotubes (BNNTs) have been theoretically predicted and later synthesised. Here we use first principles simulations to unambiguously demonstrate that i) BN nanotubes inherit the highly efficient UV luminescence of hexagonal BN; ii) the application of an external perpendicular field closes the electronic gap keeping the UV lasing with lower yield; iii) defects in BNNTs are responsible for tunable light emission from the UV to the visible controlled by a transverse electric field (TEF). Our present findings pave the road towards optoelectronic applications of BN-nanotube-based devices that are simple to implement because they do not require any special doping or complex growth.

Scientists have worked hard in the last decades to grow defect free nano-structures. The near-perfect atomic arrangement at the nano-scale has been employed to create new efficient devices as light-emitters, transistors and sensors. While many applications benefit from using defect free materials, the presence of particular impurities can generate new and fascinating properties. For example F-centre in ionic crystals have been widely used in luminescence applications¹. More recently nitrogen vacancies in diamond have been proposed for quantum computation². Defects play an important role also for the luminescence properties of hexagonal boron nitride and related nanostructures^{2–7}. Similarly to graphene, a single BN layer can be rolled up to form new structures ranging from single and multi-wall nanotubes to fullerenes^{8–12}. In contrast to graphite, the ionic character of the BN bond results in a wide band-gap of about 6 eV for bulk hexagonal-BN^{3,13,14} and excellent substrate to grow graphene for electronic applications¹⁵. The combination of such a large gap with a strong electron-hole attraction makes the optical properties of hexagonal-BN based nanostructures largely independent of the layer arrangement and dimensionality^{9,13}. Although bulk h-BN has been shown to exhibit a strong luminescence^{16,17}, it cannot be used for optical applications in the visible range because the emission frequency is fixed to about 5.75 eV in the UV. However the presence of impurities can drastically modify this scenario, as it has been shown, theoretically⁴ and experimentally^{5–7}.

The electronic structure and formation energies of the defects have been widely studied in bulk h-BN and BN nanotubes^{18–23}. Luminescence in the visible was attributed to the presence of deep levels in the sample^{24–26}, whereas the UV emission is an intrinsic response (Frenkel-exciton) of the structurally perfect hexagonal BN²⁷. Here we propose to engineer BNNTs with particular defects in order to generate light-emission in a wide range of frequencies that can be tuned by means of an external electric field. The range of tunability of the proposed nanotube-based light emitting device depends on the defect location and type.

For pure BNNTs, it has been shown that the application of a transverse electric field generates a Stark effect leading to a strong reduction of the band gap^{28,29}. The external field leads to a localisation of the conduction-band minimum/valence-band maximum on opposite sides of the tube (see Fig. 1). The corresponding energy shift of the band edges is thus proportional to the nanotube diameter. Experimentally as-grown nanotubes contain defects that lead to both deep or shallow levels in the gap. The wave-functions of these levels are, a priori, only

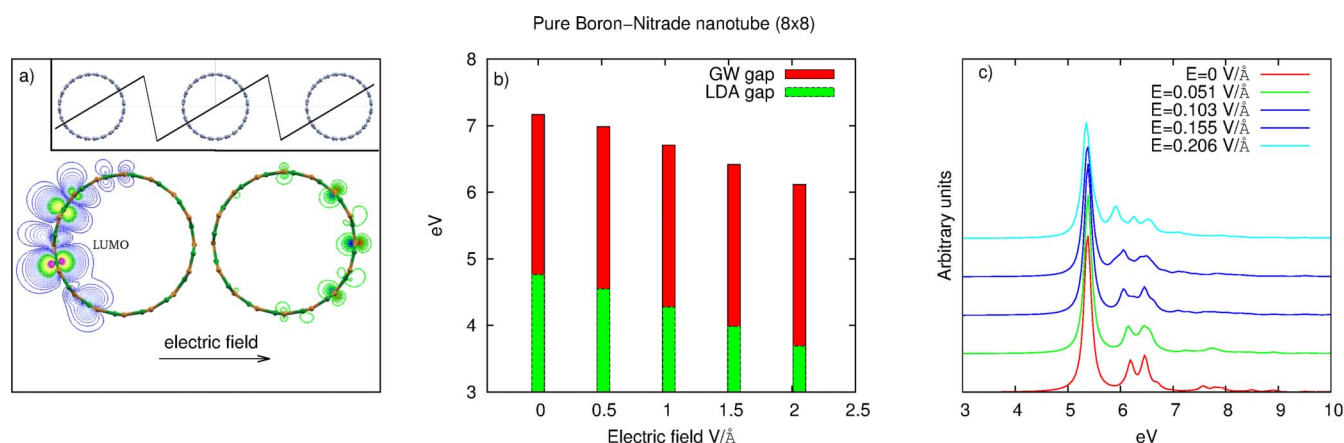


Figure 1 | Panel (a) left (right): lowest conduction band (highest valence band) in presence of an external field $E = 0.206$ V/Å. In panel (b) we report the band gap of BN 8×8 nanotube versus the TEF in LDA and G_0W_0 approximations; in panel (c) the corresponding optical absorption computed at the many-body Bethe-Salpeter level.

slightly affected by the presence of an external electric field^{22,30} because they are associated with localised orbitals centred on the impurity. However, their level position with respect to the bands edges changes^{22,30} because valence (conduction) bands are modified by the external field. Here we will show that this property can be employed to produce tunable and highly efficient bright light-emission devices based on defective BN nanotubes.

Results

We model the electronic and structural properties of the pure and defected BN nanotubes under a TEF using state-of-the-art first-principles methods based on Density Functional Theory (DFT) combined with Many-Body Perturbation-Theory (MBPT) approaches. These methods allow calculation of quasiparticle band structure and optical properties with a high degree of accuracy (see Methods section for details). In the past this theoretical framework has been shown to be very efficient in predicting the electronic properties of BN nanotubes that were later on confirmed in the experiments^{9,10,11,13}.

We start our study by analysing the case of pure isolated BN nanotubes immersed in a static transverse electric field. A transverse electric field reduces the band gap, as shown in panel (b) of Fig. 1. The gap reduction, induced by the TEF, is directly proportional to the electric field strength and to the tube diameter³¹. Surprisingly the shrinking of the band-gap slightly modifies the optical response of the tube³⁰. The main exciton remains in the same position, while a small fraction of its spectral weight is redistributed to higher excitons (see panel (c) in Fig. 1). In fact the conduction and valence orbitals contributing to the gap reduction are localised on opposite sides of the tube and they have very little overlap (see panel (a) of Fig. 1) and therefore their contribution to the optical response is negligible. We conclude that while the giant Stark effect present in BNNTs can modify their transport properties³², it leaves the optical response mainly unchanged. The light emission spectra of *pure* BNNTs is thus not tunable by an external electric field. The presence of defects drastically modifies this picture. Different experiments have shown that impurities induce light emission below 5 eV in BN nanostructures^{5–7}, and modify the luminescence arising from the main bulk exciton⁴. These effects can be explained by the presence of deep levels in the BN band gap⁴. The low frequency emissions are due to transitions from and to these levels. Moreover when the impurity levels are close to the top valence band or bottom conduction band they mix with the bulk excitations giving rise to a splitting of the main excitonic peak⁴. Among the different impurities responsible for light emission we can distinguish two families: defect complexes and single defect centres. The first family is formed by multiple defects as for instance di-vacancies, defect lines and so on. The second family

consists in a single defect centre as for instance boron (nitrogen) vacancies or a substitution of a boron (nitrogen) atom with a carbon one. The main difference between these two families lies in the different kind of transitions involved in light absorption/emission processes. In the case of defect complexes both donor and acceptor states are present in the band gap while in the other case there is only a single donor or acceptor state. Therefore in the case of defect complexes the optical response is dictated by the quasi-donor-acceptor transitions³³, while in the simple defect centres light absorption/emission is due to transitions between bulk states and deep defect levels (see Fig. 2).

The electronic structure of defects in BN nanotubes is similar to the one of defects in a single BN-sheet¹⁸. In fact due to the large band gap curvature effects play a minor role on the optical properties of pure BNNTs, where the strong localisation of excitons renders the optical spectra almost independent from the tube diameter and chirality^{13,34}. In order to simulate a tube with defects we use the same methodology employed for the pure tube but with larger supercells in such a way to reduce the defect-defect interaction. Although large part of the tubes produced in the experiments are multi-wall and possess a zig-zag chirality, we chose a 12×12 armchair one as prototype for our study. This choice is motivated by two reasons: first the primitive cell of an armchair tube, radius being equal, contains less atoms than a chiral one, second we expect only small differences with respect to the optical response of multi-wall or chiral nanotubes for the reasons discussed above. When we turn on a TEF, the band gap of the tube shrinks and consequently the defect levels change position with respect to the band edges^{22,30}. The orbitals associated with defects levels are strongly localised on the impurities (see right panel of Fig. 3) and therefore they are slightly deformed by the presence of the external field. To first order, the shift of the defect levels is thus given by the potential generated by the TEF and depends therefore on the position of the defect with respect to the direction of the electric field (see inset in Fig. 2). This is visualised in the bottom panel of Fig. 2 for three different defect positions. We will show in the following, how this property gives rise to a tunable and efficient light emission.

In order to predict the emission frequencies of BN nanotubes in presence of defects, we used a simplified approach. The first necessary ingredient to get light emission is non-vanishing optical matrix elements between the discrete donor (acceptor) state and the continuum states of the bottom conduction (top valence) bands. In the upper panel of Fig. 2 we show the strength of the optical matrix elements between the defect level and the bottom conduction bands for the case of a Boron vacancy, V_B . The optical matrix element displays a strong dependence on the angle between the defect

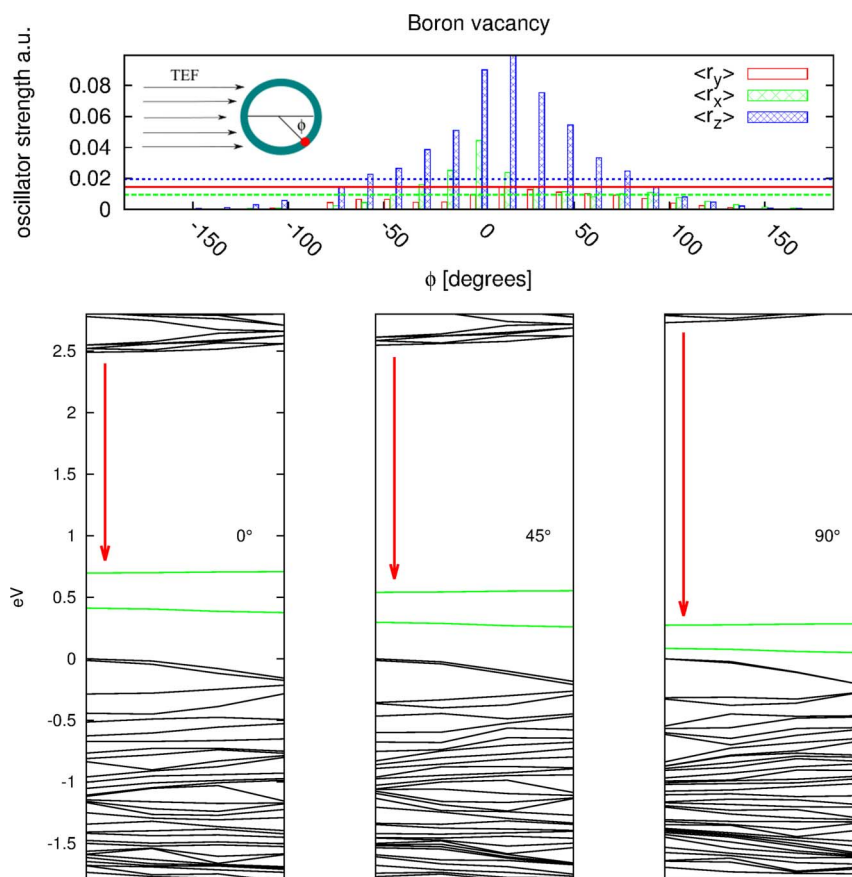


Figure 2 | In the top panel we report the oscillator strength versus the angle between the defect and the bottom conduction band for V_B . The optical matrix elements are averaged on the first conduction bands within an energy range of 0.15 eV. The straight lines are the dipole matrix elements at zero TEF. In the same figure it is present also a schematic representation of the a BN tube with a defect in presence of a TEF. In the bottom panels we show the band structure of the same tube versus the angle between the defect and the electric field. The red arrow represents the transition responsible for the luminescence in presence of V_B . The intensity of the TEF is 0.206 V/Å.

position and the electric field (see inset in the top panel of Fig. 2). The same phenomena occurs for other simple acceptor or donor defects like substitution of a Nitrogen or a Boron atom by a carbon one, C_B and C_N respectively. Furthermore, we note that the optical matrix

elements for polarisation along the tube axis (z-axis) dominate, which also holds for the optical response of pure nanotubes⁹.

The presence of the external electric field localises valence and conduction bands on opposite sides of the tube (see Fig. 1), therefore

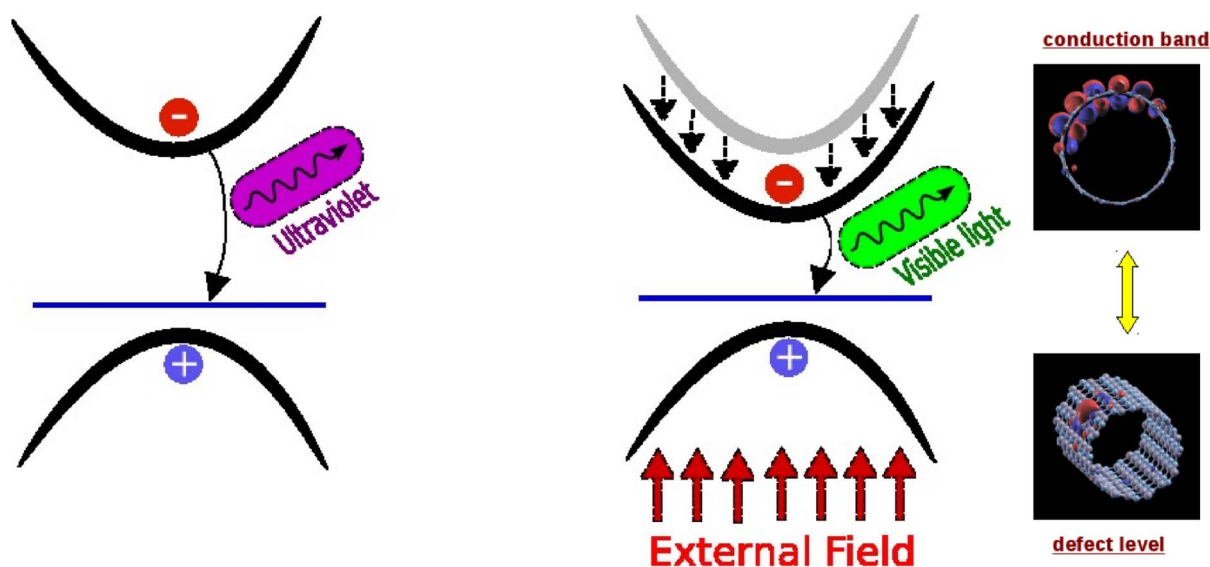


Figure 3 | Schematic representation of light emission process for an acceptor impurity in a BN nanotube. On the left a simplified band structure picture in presence of a TEF. On the right conduction and defect orbitals responsible for the emission process.



transitions are maximal only when the defect is aligned with the bottom (top) of the conduction (valence) band. The dipole element decreases to almost zero as the defect is moved to the opposite side of the tube. Consequently one can expect that luminescence, which is generated by transitions from and to the defects levels, will be efficient only when the defects are positioned on the side of the “localised” conduction (valence) band edge. This focusing effect increases with the tube size and field intensity.

Now that we are sure that transitions from and to simple defect centres are not zero in presence of a transverse electric field, we investigate how the field modifies the emission frequencies. In order to predict light emission we start from the quasi-particle (QP) band structure in presence of defects. We consider the energy differences for transitions between defect states and the top valence (bottom conduction) states. This allows us to investigate light-emission versus transverse electric field, without including electron-hole interaction or lattice relaxation (see Methods section). We found that also in presence of defects the GW renormalisation for conduction (valence) bands and defects levels is almost a constant with respect to the external electric field (see also Fig. 1(b)).

Luminescence can be estimated from the QP band structure in presence of TEF as the sum of independent transitions between conduction bands and defect states. However light emission originates from electron-hole recombination, a two-particle process that cannot be described by means of the quasi-particle band structure only. In fact electrons and holes attract each other and this attraction modifies the transition energies. These processes can be naturally treated within a two-particle Green's functions formalism³⁵ and it has been shown that transition energies from and to defect states are strongly renormalised⁴ by the electron-electron correlation. In order to model this correction, we calculate the exchange and electron-hole attraction between the defect level and the bottom conduction (top valence) bands only. In the past this approximation has been successfully employed to predict excitation energies of F-colour centres³⁶.

In addition to the corrections originating from the electronic correlation, we have to consider the contributions due to the lattice relaxation induced by the excited carriers. These are the so called Stokes and anti-Stokes shifts. The Stokes shift can be estimated by means of a constrained DFT calculation with different defect occupation. We investigated three different defects, an acceptor, the Boron vacancy V_B , a donor, the Carbon substitution of a Boron atom C_B , and the Boron-Nitrogen di-vacancy V_{BN} . In order to estimate the Stokes shift we considered the case of a completely empty acceptor state (or a completely filled donor state). In principle one should consider also the correction coming from the partial filling (emptying) of the conduction (valence) bands, but this is supposed to be a minor effect because these bands are delocalised along the z direction. In this way we obtain a rough estimation of the Stokes shift of $\Delta E_s \simeq 0.19$ eV for C_B and $\Delta E_s \simeq 0.03$ eV for V_B . We did not calculate any Stokes shift for V_{BN} because in this case it is irrelevant as it

will be clear in the following. Vested with this theoretical approach we proceed in the study of light emission versus the external electric field.

We report our predicted light emission for $BN(12, 12)$ tube versus the transverse electric field in Fig. 4. As one can see from the figure an external electric field allows to vary the emission frequency in a large spectral range for the C_B and V_B cases. Notice that in presence of defect complexes, as for instance the BN di-vacancy V_{BN} , the emission frequency does not change with the external field. In fact in this case the emission is dominated by transitions between donor and acceptor states in the band-gap^{4,33}. Since the wave-functions associated to these states are localised on the impurity, the effect of external electric field is irrelevant. In the left panel of Fig. 3 we show a scheme of the light emission process from BN nanotubes in presence of defects. We want to underline that this process happens only when the defect is aligned with the conduction (valence) maximum, otherwise the emission will be inefficient due to the small dipole matrix elements.

Although the results of Fig. 4 can be theoretically extended to larger tubes, calculations become soon prohibitive due to the large number of atoms, the vacuum in the super-cell and the number of conduction bands that enter in the many-body operators. Therefore in order to predict light emission in larger (more realistic) tubes we assume many-body corrections to be a constant with respect to the tube size and we fit the emission energy with a simple linear curve

$$E_{\text{emission}} = E_0 + \alpha \zeta \quad (1)$$

where ζ is the external electric field. This relation was already employed to describe the band gap closing of h-BN nanotubes under the effect of a TEF in simple tight-binding models and *ab-initio* calculations^{31,37}. In principle the linear coefficient α depends on the tube size. In order to estimate this dependence we performed different calculations at the DFT level, varying the tube size. We found that α changes linearly with the tube radius R , $\alpha(R) = \alpha_0 + R\beta$. A similar behaviour has been found for the pure BNNTs gap versus the electric-field and tube radius³¹. Combining the previous two equations we can predict the electric field ζ necessary to produce light emission at a given frequency E_1 :

$$\zeta = \frac{E_1 - E_0}{\alpha_0 + R\beta} \quad (2)$$

Now we use Eq. 2 to estimate the intensity of the TEF that will induce emission in the visible range (1.65–3.1 eV). In Fig. 5 we report the visible emission range for the V_B and C_B cases versus the TEF intensity and tube radius.

In general an increase of the tube size reduces the strength of the transverse electric field necessary to obtain emission in the visible range. For sufficient large tubes the TEF intensity is of the same order of the one available in small devices. Notice that a TEF produces an electrostatic potential inside the tube that is proportional to the TEF

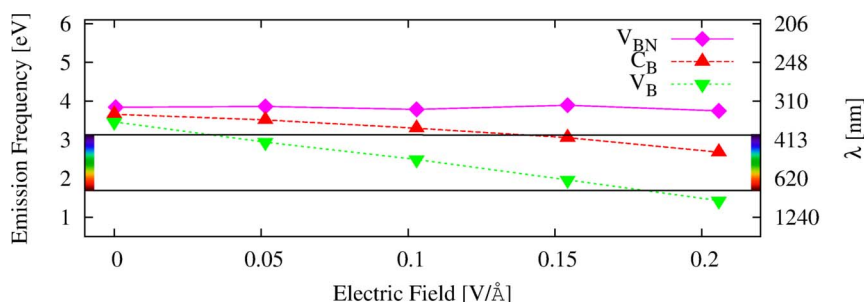


Figure 4 | Predicted light emission for different defects as a function of the transverse electric field. All the defects are taken in the position of maximum emission, according to their optical matrix elements, see also Fig. 2. In the V_{BN} we did not include any Stokes shift.

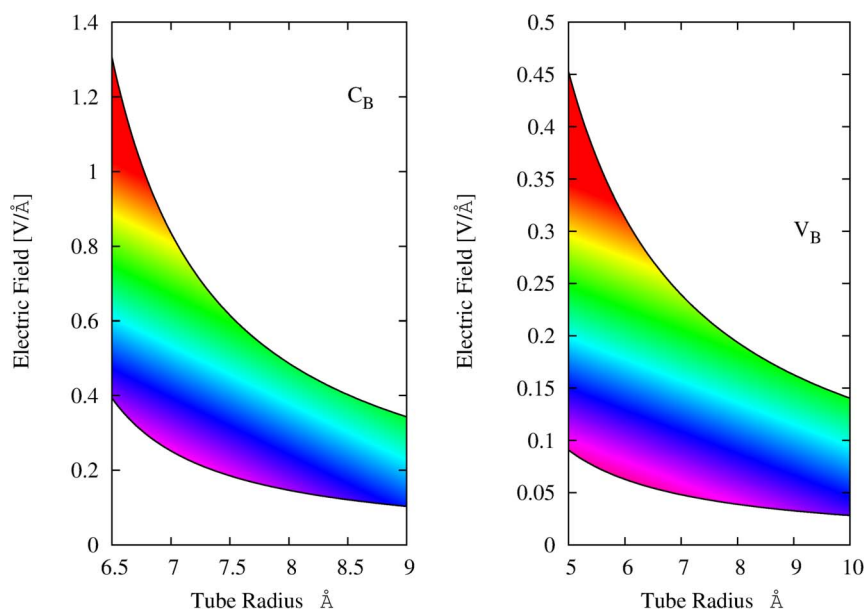


Figure 5 | Visible light emission range as function of the tube radius and the external electric field for V_B and C_B cases (rainbow colours are just a guide to the eyes).

intensity and the tube radius²². Therefore Eq. 2 breaks down for too large nanotubes or too strong fields. However a giant Stark effects has been experimentally measured in pure BN nanotubes with a radius of about 23 Å and a TEF of 0.08 V/Å. In the same experiment a gap reduction of more than 1 eV has been obtained²⁹. Comparing these values with our extrapolation in Fig. 5 it is clear that there is a large margin to produce visible light with experimentally accessible nanotubes and electric fields.

Finally we consider defect formation and their charge state. Recent experiments³⁸ have shown that it is possible to introduce defects in h-BN structures by means of electron irradiation. This process is mainly dominated by boron mono-vacancies even if other larger vacancies are present. These vacancies can also be transformed in substitutional defects by introducing C atoms in the experiment^{39,40}, and the final process can be controlled by charging the system during the irradiation⁴⁰. These advances make possible the realisation of the device that we are going to discuss in the following. Regarding the charge state of the defects, in the present paper we investigated only neutral ones. Charged defects possess different relaxation energies and electronic structure. This fact influences also their optical properties, as it has been recently shown in the case of vacancies in SiC⁴¹. The present results can easily be extended to charged defects and we expect that the main findings will remain valid. In fact the tunability of the light emission is related to the localisation of defect states versus the delocalised bulk ones. Therefore a different charge state

will modify the emission at zero field but not its behaviour in presence of a TEF.

Now that we have shown how to produce tunable light emission with defective BN nanotubes and discussed the feasibility of our idea, we briefly present the possible configurations of a device based on BN nanotubes. The generic configuration of the device (see Fig. 6) comprises depositing as-grown BN nanotubes on an insulating surface (for example silicon oxide) acting as a dielectric to enable the application of the gated electric field that controls the light emission. The configurations is very much similar to the one of a field effect transistor (FET). The activation of the BN-defected optoelectronic device could be done by one of the following three processes: i) using UV light, ii) introducing an ambipolar current that recombines at the defect and emits light dictated by the applied gate voltage⁴² iii) using tunnelling current through an STM tip close to the nanotube. The excited electrons would inelastically decay very fast into the lowest energy state (the defect-like Frenkel exciton) that would further decay by emitting light, again with a frequency dictated by the applied voltage, a process similar to the one leading to light emission in electronically excited semiconductors and fluorescent materials. A schematic set-up of those devices is illustrated in Fig. 6.

Discussion

In conclusion, we have shown that light emission from BNNTs with simple defect centres can be tuned by the presence of a transverse

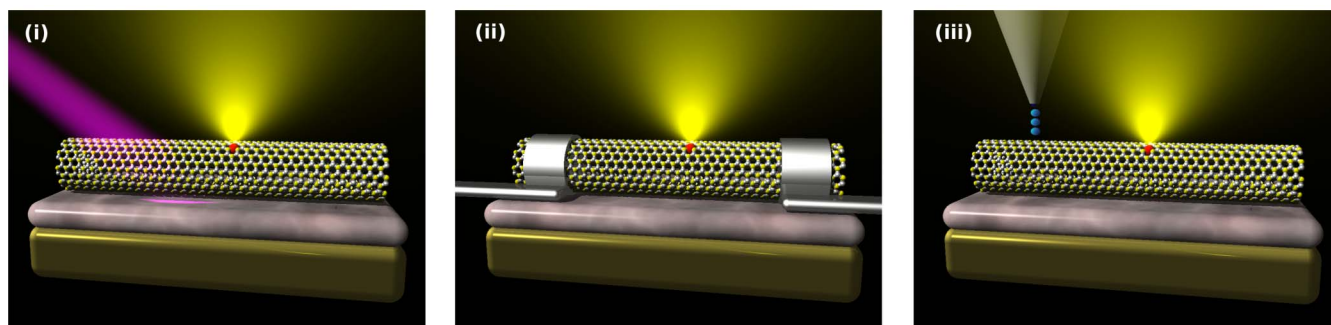


Figure 6 | Schematic set-up for the suggested three possibilities to activate the optoelectronic device based on defective BN nanotubes (i) light-induced luminescence (ii) ambipolar transistor configuration (iii) electron induced electron-hole pairs by means of STM tip.



electric field. This opens the possibility to use these systems as light emitting devices. The use of (non-tunable) UV-light emitting devices based on crystalline hexagonal BN has already been suggested before⁴³. Here, we move one important step further by showing how nanotube based devices could operate in the UV and visible range by varying the external field. The external electric field, necessary to tune the emission, can be applied using a field-effect transistor configuration³². The intensity necessary to produce visible light decreases with the tube size. The present results have been patented by some of the authors⁴⁴.

Finally we envision that the present findings can be applied to other two-dimensional semiconducting or insulating layered materials that form tubes, as it is the case for transition metal dichalcogenides⁴⁵.

Methods

BNNTs are simulated by using a supercell approach¹¹, where the tube is oriented along the z direction, and a large empty space is left in the other two directions between tube replica in order to reduce the tube-tube interactions. Subsequently a sawtooth electric field (see inset in Fig. 1(a)) with the cell periodicity is added along the x direction. In order to simulate light emission in BNNTs we employed a combination of Density-Functional Theory (DFT) plus Many Body Perturbation Theory (MBPT). DFT is an exact theory for ground state properties and it is known to describe very well the structural properties of boron-nitride nanostructures within Local Density Approximation (LDA). All DFT calculations have been performed using a $1 \times 1 \times 5$ supercell containing 240 atoms. The distance between the tube replica was 29 a.u., we used a $1 \times 1 \times 2$ k-point sampling, LDA for the exchange correlation functional⁴⁶, a plane waves cutoff of 45 Ry for the wave-function and norm-conserving pseudo-potentials⁴⁷. All DFT calculations have been performed with the PWSCF code⁴⁸ and the atomic structures have been relaxed using a BFGS quasi-Newton algorithm. Excited state and optical properties have been studied by means of MBPT. We calculated quasi-particle properties solving a Dyson equation within the so-called G_0W_0 approximation^{49,50}, where all the Green's functions and the self-energy operator are constructed with eigenvalues and eigenvectors of the Kohn-Sham(KS) Hamiltonian. Non-self consistent GW calculations have been performed with the code YAMBO⁵¹ using a plasmon pole approximation for the dielectric constant. We used 30,000 G-vectors for the wave-function, 2 Ha for the response block size and 3000 bands for the screening. A cylindrical cutoff has been applied to the Coulomb potential in order to reduce the tube-tube interaction. Neutral excitations, responsible for the absorption spectra were obtained from a two-particle Green's function equation, the Bethe-Salpeter equation, that is solved in the static ladder approximation³⁵, including excitonic effects. We excluded quasi-free electron states²⁸ in the Bethe-Salpeter equation, because they are not supposed to be responsible for luminescence. We performed all calculations without including spin-polarisation effects. Even if we know that exchange-splitting slightly modifies the defect levels positions^{45,52}, this effect does not modify the main results of the paper. For the large tubes employed to get the results in Fig. 4 we estimated the GW and electron-hole interaction from the one of a BN-sheet with the same defects and a distance between the periodic replica equal to the inter-tube distance⁴.

- Seitz, F. Color centers in alkali halide crystals. *Rev. Mod. Phys.* **18**, 384–408 (1946).
- Barrett, S. D. & Kok, P. Efficient high-fidelity quantum computation using matter qubits and linear optics. *Phys. Rev. A* **71**, 060310 (2005).
- Wirtz, L. *et al.* Comment on “huge excitonic effects in layered hexagonal boron nitride”. *Phys. Rev. Lett.* **100**, 189701 (2008).
- Attacalite, C., Bockstedt, M., Marini, A., Rubio, A. & Wirtz, L. Coupling of excitons and defect states in boron-nitride nanostructures. *Phys. Rev. B* **83**, 144115 (2011).
- Silly, M. G. *et al.* Luminescence properties of hexagonal boron nitride: Cathodoluminescence and photoluminescence spectroscopy measurements. *Phys. Rev. B* **75**, 085205 (2007).
- Jaffrennou, P. *et al.* Near-band-edge recombinations in multiwalled boron nitride nanotubes: Cathodoluminescence and photoluminescence spectroscopy measurements. *Phys. Rev. B* **77**, 235422 (2008).
- Museum, L., Feldbach, E. & Kanaev, A. Defect-related photoluminescence of hexagonal boron nitride. *Phys. Rev. B* **78**, 155204 (2008).
- Pakdel, A., Zhi, C., Bando, Y. & Golberg, D. Low-dimensional boron nitride nanomaterials. *Mater. Today* **15**, 256–265 (2012).
- Wirtz, L. & Rubio, A. Optical and vibrational properties of boron nitride nanotubes. In *BCN Nanotubes and Related Nanostructures*, 105–148 (Springer, 2009).
- Ayala, P., Arenal, R., Loiseau, A., Rubio, A. & Pichler, T. The physical and chemical properties of heteronanotubes. *Rev. Mod. Phys.* **82**, 1843–1885 (2010).
- Rubio, A., Corkill, J. L. & Cohen, M. L. Theory of graphitic boron nitride nanotubes. *Phys. Rev. B* **49**, 5081 (1994).
- Chopra, N. G. *et al.* Boron nitride nanotubes. *Science* **269**, 966 (1995).
- Wirtz, L., Marini, A. & Rubio, A. Excitons in boron nitride nanotubes: Dimensionality effects. *Phys. Rev. Lett.* **96**, 126104 (2006).
- Arnaud, B., Lebegue, S., Rabiller, P. & Alouani, M. Huge excitonic effects in layered hexagonal boron nitride. *Phys. Rev. Lett.* **96**, 026402 (2006).
- Dean, C. R. *et al.* Boron nitride substrates for high-quality graphene electronics. *Nat. Nanotechnol.* **5**, 722 (2010).
- Watanabe, K., Taniguchi, T. & Kanda, H. Direct-bandgap properties and evidence for ultraviolet lasing of hexagonal boron nitride single crystal. *Nat. Mater.* **3**, 404 (2004).
- Kubota, Y., Watanabe, K., Tsuda, O. & Taniguchi, T. Deep ultraviolet light-emitting hexagonal boron nitride synthesized at atmospheric pressure. *Science* **317**, 932 (2007).
- Schmidt, T. M., Baierle, R. J., Piquini, P. & Fazzio, A. Theoretical study of native defects in bn nanotubes. *Phys. Rev. B* **67**, 113407 (2003).
- Liu, R., Li, J. & Zhou, G. Ab initio investigation about the possibility of ferromagnetism induced by boron vacancy in bn nanotubes. *J. Phys. Chem. C* **114**, 4357–4361 (2010).
- Kang, H. S. Theoretical study of boron nitride nanotubes with defects in nitrogen-rich synthesis. *J. Phys. Chem. B* **110**, 4621–4628 (2006).
- Zhukovskii, Y. F., Bellucci, S., Piskunov, S., Trinkler, L. & Berzina, B. Atomic and electronic structure of single-walled BN nanotubes containing N vacancies as well as C and B substitutes of N atoms. *Eur. Phys. J. B* **67**, 519–525 (2009).
- Hu, S., Li, Z., Zeng, X. C. & Yang, J. Electronic structures of defective boron nitride nanotubes under transverse electric fields. *J. Phys. Chem. C* **112**, 8424–8428 (2008).
- Zobelli, A. *et al.* Defective structure of bn nanotubes: From single vacancies to dislocation lines. *Nano Lett.* **6**, 1955–1960 (2006).
- Chen, H. *et al.* Eu-doped boron nitride nanotubes as a nanometer-sized visible-light source. *Adv. Mater.* **19**, 1845–1848 (2007).
- Han, W.-Q. *et al.* Isotope effect on band gap and radiative transitions properties of boron nitride nanotubes. *Nano Lett.* **8**, 491–494 (2008).
- Chen, H., Chen, Y. & Liu, Y. Cathodoluminescence of boron nitride nanotubes doped by ytterbium. *J. Alloy Compd.* **504**, S353–S355 (2010).
- Pierret, A. *et al.* Excitonic recombinations in hBN: from bulk to exfoliated layers. *arXiv preprint arXiv 1306.2850* (2013).
- Khoo, K. H., Mazzoni, M. S. C. & Louie, S. G. Tuning the electronic properties of boron nitride nanotubes with transverse electric fields: A giant dc Stark effect. *Phys. Rev. B* **69**, 201401 (2004).
- Ishigami, M., Sau, J. D., Aloni, S., Cohen, M. L. & Zettl, A. Observation of the giant Stark effect in boron-nitride nanotubes. *Phys. Rev. Lett.* **94**, 056804 (2005).
- Attacalite, C., Wirtz, L., Marini, A. & Rubio, A. Absorption of bn nanotubes under the influence of a perpendicular electric field. *Phys. Status Solidi B* **244**, 4288–4292 (2007).
- Zheng, F., Liu, Z., Wu, J., Duan, W. & Gu, B.-L. Scaling law of the giant stark effect in boron nitride nanoribbons and nanotubes. *Phys. Rev. B* **78**, 085423 (2008).
- Radosavljević, M. *et al.* Electrical properties and transport in boron nitride nanotubes. *Appl. Phys. Lett.* **82**, 4131–4133 (2003).
- Museum, L. & Kanaev, A. Near band-gap photoluminescence properties of hexagonal boron nitride. *J. Appl. Phys.* **103**, 103520 (2008).
- Park, C.-H., Spataru, C. D. & Louie, S. G. Excitons and many-electron effects in the optical response of single-walled boron nitride nanotubes. *Phys. Rev. Lett.* **96**, 126105 (2006).
- Strinati, G. Application of the greens functions method to the study of the optical properties of semiconductors. *Riv. Nuovo Cimento* **11**, 1 (1988).
- Chacham, M. P. S. H. & Louie, S. G. Quasiparticle excitation energies for the F-center defect in LiCl. *Phys. Rev. B* **51**, 7464 (1995).
- Chegel, R. & Behzad, S. Electro-optical properties of zigzag and armchair boron nitride nanotubes under a transverse electric field: Tight binding calculations. *J. Phys. Chem. Solids* **73**, 154–161 (2012).
- Jin, C., Lin, F., Suenaga, K. & Iijima, S. Fabrication of a freestanding boron nitride single layer and its defect assignments. *Phys. Rev. Lett.* **102**, 195505 (2009).
- Krivanek, O. L. *et al.* Atom-by-atom structural and chemical analysis by annular dark-field electron microscopy. *Nature* **464**, 571–574 (2010).
- Berseneva, N., Krashennnikov, A. V. & Nieminen, R. M. Mechanisms of postsynthesis doping of boron nitride nanostructures with carbon from first-principles simulations. *Phys. Rev. Lett.* **107**, 035501 (2011).
- Bockstedt, M., Marini, A., Pankratov, O. & Rubio, A. Many-body effects in the excitation spectrum of a defect in sic. *Phys. Rev. Lett.* **105**, 026401 (2010).
- Chen, J. *et al.* Bright infrared emission from electrically induced excitons in carbon nanotubes. *Science* **310**, 1171–1174 (2005).
- Taniguchi, T., Watanabe, K., Kubota, Y. & Tsuda, O. Production of a hexagonal boron nitride crystal body capable of emitting out ultraviolet radiation (2010). Patent number: US 2010/0120187 A1.
- Rubio, A., Attacalite, C. & Wirtz, L. Light emitting source and method for emitting light based on boron nitride nanotubes (2012). Patent number: WO/2012/113955.
- Wang, Q. H., Kalantar-Zadeh, K. A., Kis, A., Coleman, J. N. & Strano, M. S. Electronics and optoelectronics of two-dimensional transition metal dichalcogenides. *Nat. Nano* **7**, 699 (2012).
- Ceperley, D. M. & Alder, B. J. Ground state of the electron gas by a stochastic method. *Phys. Rev. Lett.* **45**, 566 (1980).
- Troullier, N. & Martins, J. L. Efficient pseudopotentials for plane-wave calculations. *Phys. Rev. B* **43**, 1993 (1991).



48. Giannozzi, P. *et al.* Quantum espresso: a modular and open-source software project for quantum simulations of materials. *J. Phys. Condens. Matter* **21**, 395502 (2009).
49. Aryasetiawan, F. & Gunnarsson, O. The GW method. *Rep. Prog. Phys.* **61**, 237 (1998).
50. Strinati, G., Mattheus, H. J. & Hanke, W. Dynamical correlation effects on the quasiparticle Bloch states of a covalent crystal. *Phys. Rev. Lett.* **45**, 290–294 (1980).
51. Marini, A., Hogan, C., Gruning, M. & Varsano, D. Yambo: an ab initio tool for excited state calculations. *Comp. Phys. Comm.* **180**, 1392 (2009).
52. Liu, R.-F. & Cheng, C. Ab initio studies of possible magnetism in a *bn* sheet by nonmagnetic impurities and vacancies. *Phys. Rev. B* **76**, 014405 (2007).

Acknowledgements

We acknowledge financial support also from the European Research Council Advanced Grant DYNamo (ERC-2010-AdG-267374), Spanish Grant (FIS2010-21282-C02-01), Grupos Consolidados UPV/EHU del Gobierno Vasco (IT578-13), Ikerbasque and the European Commission project CRONOS (Grant number 280879-2). Computational time

was granted by i2basque and BSC Red Espanola de Supercomputacion and GENCI-IDRIS (Nos. 100063 and No. 091827). A. M. acknowledges funding by MIUR FIRB Grant No. RBFR12SW0J.

Author contributions

C.A., L.W., A.M. and A.R. contributed to the discussions, theoretical analysis and writing of the manuscript. C.A. performed the calculations and A.R. designed the research.

Additional information

Competing financial interests: The authors declare no competing financial interests.

How to cite this article: Attacalite, C., Wirtz, L., Marini, A. & Rubio, A. Efficient Gate-tunable light-emitting device made of defective boron nitride nanotubes: from ultraviolet to the visible. *Sci. Rep.* **3**, 2698; DOI:10.1038/srep02698 (2013).



This work is licensed under a Creative Commons Attribution 3.0 Unported license. To view a copy of this license, visit <http://creativecommons.org/licenses/by/3.0>